

RESEARCH ARTICLE

Examination of Experimental and Theoretical Behavior of a Reinforced Concrete Room under Internal Explosion Loads

Yusuf Demirel, Ömer Polat

Gazi University, Engineering Faculty, Civil Engineering Department, 06560 Ankara, TURKEY

The Scientific and Technical Research Council of Turkey, 06560 Ankara, TURKEY

Abstract

The present study reports on an experimental investigation of the effect of a blast inside a reinforced concrete room on the behavior of the reinforced concrete structure. To this end, a blasting experiment was carried out inside a concrete room, with pressure values obtained using a piezoelectric pressure sensor. After the experiment, measurements and observations were made within the reinforced concrete room, and sketches were made of the cracks that formed on the various concrete wall types, and on the floor and wall coverings. The gathered data, measurements and observations were then used in a theoretical study. The obtained pressure values were used to analyze the effects of the blast on the room components, making use of ABAQUS software, with both dynamic and static analyses conducted separately. The results of the theoretical study of the behavior of the building components, which was carried out in accordance with international regulations and standards, were then compared with the experimental values.

Keywords: Internal explosion, Reinforced concrete room, Experiment, Crack sketch, Opening

1) Introduction

When designing military, civilian and industrial structures, knowledge of the impacts of blasts inside structures resulting from terrorist attacks or accidents, as well as of the behavior of the structure under blast loads, is crucial. It is important that the stability of a structure is maintained in the event of an internal blast. The damage and loss of life resulting from blasts within buildings have increased in recent years. It is therefore important to know how a building will behave, how the stability of the building will be affected and how much damage the structure will sustain in the event of an internal blast.

Blasts occurring inside structures lead to impacts, expansions and thrusts involving complex waveforms. The complex pressure waves that form as a result of an internal blast comprise the reflecting shock waves that are produced within the structure and the gases that accumulate as a result of the blast [1]. The internal blast loads given by Beshara [1] and presented in Figure 1 are the shock waves that are produced from the reflections of the initial pressure, as well as the gas pressure, i.e. the quasi-static gas pressure, which lasts longer than the shock pressures, and forms due to accumulation of gas waste. Reflected shock pressure waves are larger but do not last as long as quasi-static gas pressure waves [2].

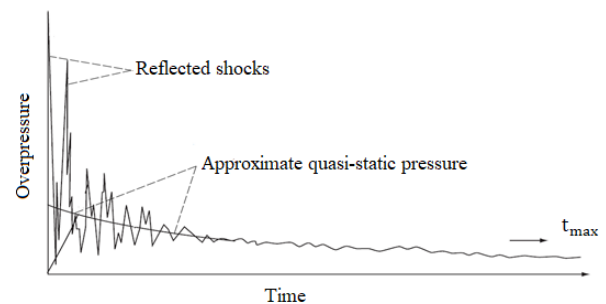


Figure 1. Typical internal blast pressure-time graph [2]

In the present study, two different approaches are developed that simplify the calculation of internal blast pressures. In the first approach, Baker's proposal [3] was used, as shown in Figure 2, featuring a model in which three shock pressures are generated as a result of the blast, with the magnitude of pressure falling by half at each reflection. t_a refers to the time it takes for the shock pressure to reach the structural element, whereas t_r refers to the time of the idealized shock pressure, which is equal to twice t_a [3]. Quasi-static gas pressures are not considered in this approach so as to simplify the modeling.

*Corresponding Author: ydemirel@gazi.edu.tr
(Y. Demirel Orcid:0000-0002-0056-4952)

Received 10 July 2020 Revised 26 July 2020 Accepted 27 July 2020
Civil Engineering Beyond Limits 4 (2020) 20-27
2687-5756 © 2019 ACA Publishing. All rights reserved.

<https://doi.org/10.36937/cebel.2020.004.004>

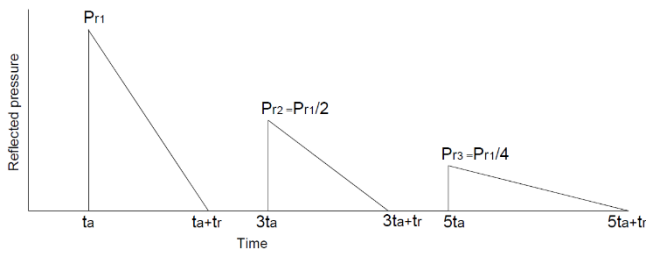


Figure 2. Reflected pressure-time graph idealized by Baker [3]

Cormie et al. proposed two graphs for P_r shock pressure and the t_a time it takes for the shock pressure to reach the component used in Baker's approach [4]. Through the use of the variables "amount of explosive" and the "distance of explosive" in these graphics, the P_r and t_a values can be obtained.

The second approach is the idealization method prescribed in UFC 3-340-2 "Structures to Resist the Effects of Accidental Explosions" [5]. This approach is based on the form and dimensions of the structure and the amount and location of explosives [5].

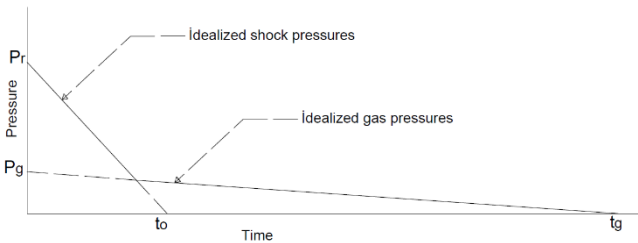


Figure 3. Internal blast pressure-time graph idealized according to UFC 3-340-02 "Structures to Resist the Effects of Accidental Explosions" [5]

When calculating the internal blast loads according to UFC 3-340-02 "Structures to Resist the Effects of Accidental Explosions" [5], it is assumed that these loads will propagate uniformly. That said, in an experimental study by Feldgun et al. in which shock pressures were measured simultaneously at nine different locations on an existing wall, it was found that the loads on the walls caused by the internal blast were not uniform [8]. Furthermore, the studies by Haskett [6], Yaoa [7,8] and Tai [9] focus on many structural parameters that have not been considered previously when investigating the effects on structures of the shock loads associated with internal blasts. The studies by Haskett [6], Yaoa [7,8] and Tai [9] experimentally and theoretically investigated the effects of blast shock waves on load-bearing systems, focusing on such parameters as the dimensions of the building, the thickness of the wall of the structure affected by the blast shock wave, the type of explosive, the shape of the explosive and the distance of the explosive from the wall. In the theoretical model provided by Y. S. Tai et al. [9], it was observed that the greater is the distance between the explosive and the load-bearing reinforced concrete structural element, the less the damage. There are several standards applied to the design of structures based on their blast loads, including the UFC 3-340-1 (2002) Design and Analysis of Hardened Structure Conventional Weapons Effects [2] and the UFC 3-340-2 (2008) Structures to Resist the Effects of Accidental Explosions [5] in the United States, the AASTP-1 (2010) Manual of NATO Safety Principles for the Storage of Military Ammunition and Explosives [10] applied by NATO, the Eurocode EN 1991-1-7 (2006) Actions on Structures [11] introduced by the European Union, and the IS 4991 (2003) Criteria for Blast Resistant Design of Structures for Explosions Above Ground [12], promulgated by the Government of India. These standards were, however, examined only for informational purposes in the evaluation of the data obtained in this study, since they are for design purposes.

2. Experimental Study

2.1. Experiment Setup

In the planned study, data in the form of measurements, as well as observations of the effects on the structural elements of an experimental internal blast within a concrete structure, were used for an analytical study.

The reinforced concrete room used for the experimental study had internal dimensions of 600 cm (w), 700 cm (l) and 400 cm (h). Considering that there is always at minimum a door and a window in any indoor environment, similar volumetric openings were created in our experiment setup to ensure that the behavior of the room modeled for the blast experiment mirrored that of a real room. Accordingly, a door opening measuring 100x220 cm was created on the right side of the measurement wall at a distance of 50 cm to the wall, along with a window opening measuring 100x100 cm, 100 cm from the floor and 250 cm from the left side of the measurement wall. Furthermore, an opening measuring 50x50 cm was created through the wall to the right of the measurement wall that was fitted with blast-resistant glass, through which video recordings were made before, during and after the experiment (Figure 6).

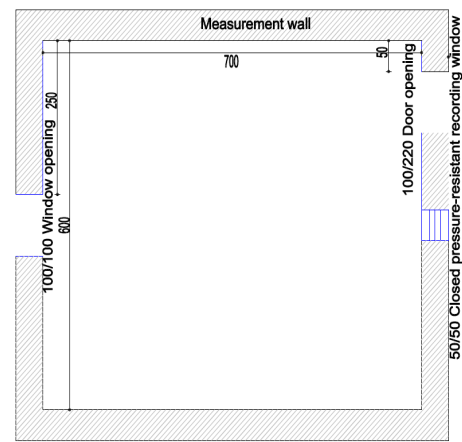


Figure 4. Plan of the reinforced concrete room built for the blast experiment

C30/37 class concrete and S420 class ribbed reinforcement were used for the construction of the reinforced concrete room. The raft foundation of the reinforced concrete room was 50 cm thick (Figure 5). The measurement wall and the other walls, referred to as the reinforced walls, were 50 cm thick and reinforced as shown in Figure 6. It was considered appropriate to include additional stirrup reinforcement to increase the resistance to the stress concentrations occurring at the edges of the walls of the structure (Figure 6). The reinforcement plan of the ceiling (50 cm thick) of the reinforced concrete room is shown in Figure 7.

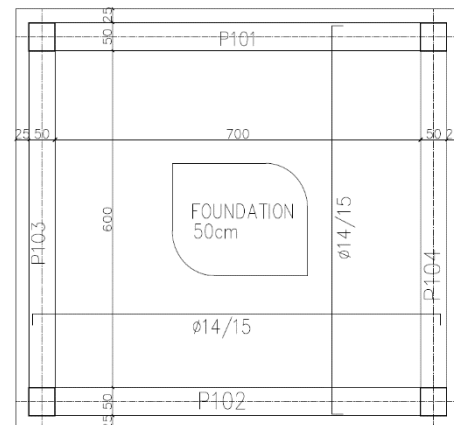


Figure 5. Reinforcement plan of the raft foundation

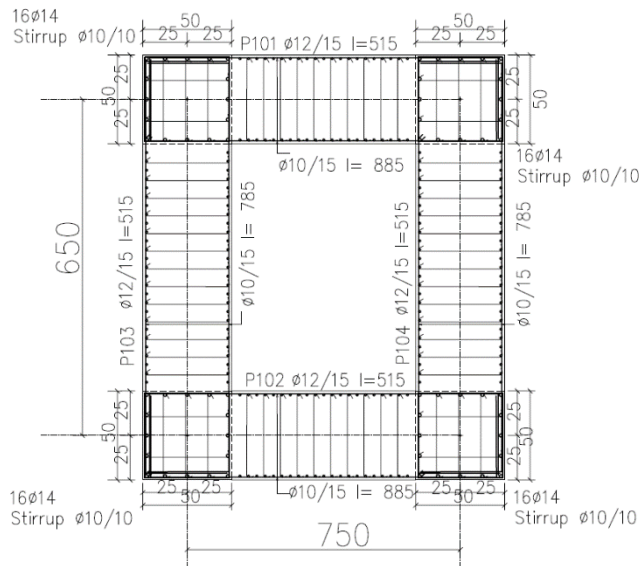


Figure 6. Reinforcement plan of the strong wall

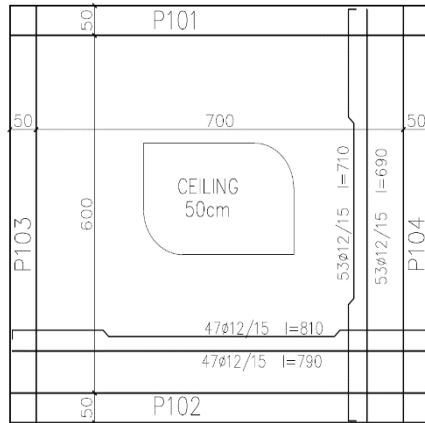


Figure 7. Reinforcement plan of the reinforced concrete room

The reinforced concrete room in which the blast experiments were carried out is shown in Figure 8. A 15 cm diameter hole was opened at the exact center (i.e. central both vertically and horizontally) of the measurement wall for the mounting of the piezoelectric pressure sensor.



Figure 8. Side view of the reinforced concrete room built for the blast experiments

The specifications of the TNT explosive selected for the study are given in Table 1, which was to be detonated with an electric fuse. A PCB ICP 113b27-series piezoelectric pressure sensor was used to measure the pressure values produced by the blast. The specifications of the sensor are given in Table 2. The pressure wave measurements recorded by the piezoelectric pressure sensor were

transferred to the IMC Cronosflex data collection device via connection cables, and pressure-time graphs were created based on the recorded data.

Table 1. Specifications of the TNT used in the experiment

TNT	Specifications
Weight	1000 g
Energy	5,569 Kj/Kg
Shape	Spherical
Speed	6,850 m/s

Table 2. Specifications of the pressure sensor used in the experiment

Performance	Value
Measurement Range (for ± 5 V output)	6.894 bar
Useful Range	13.788 bar
Sensitivity	725 mV/bar
Maximum Pressure	68.95 bar
Resonance Frequency	≥ 500 KHz
Rise Time	$\leq 1 \mu s$
Low Frequency Response (-5%)	0.5 Hz
Nonlinearity	≤ 1 %FS

2.2. Experiment Stage and the Garnered Data

For the blast experiment, 1,000 g of TNT was placed at a point 250 cm from the wall in which the pressure sensor was located at a height 200 cm from the floor and 350 cm from the room edges, aligned precisely with the window opening and the blast-resistant observation window. The pressure-time graph, produced based on the data obtained from the piezoelectric pressure sensor for the explosion of 1000 g of TNT at a distance 250 cm from the measurement wall, is given in Figure 9.

An evaluation of the data indicated pressure-time pressure lasting for 0.105 s, with the first pressure wave reaching the piezoelectric pressure sensor in 0.00018 s. The maximum shock pressure measured in the blast experiment was 0.84 MPa, which was reached 0.0016 seconds after the blast.

As a result of the blast, no rupture or permanent deformation was observed on the inner or outer surfaces of the reinforced walls or the ceiling, although some areas of the reinforced walls were blackened. After cleaning the surface of the reinforced walls with a wire brush, capillary cracks were observed to have formed in the areas where the inner and outer surfaces of the reinforced walls meet the raft foundation. It was found also that cracks had formed at the edges of the door and window openings. Further cracks were found to extend from the center of the ceiling to the corners. It was not possible to make any observations during the blast, since the blast duration was too short. The form and length of the cracks observed in the reinforced concrete room following the blast are shown in the sketches given in Figures 10 and 11.

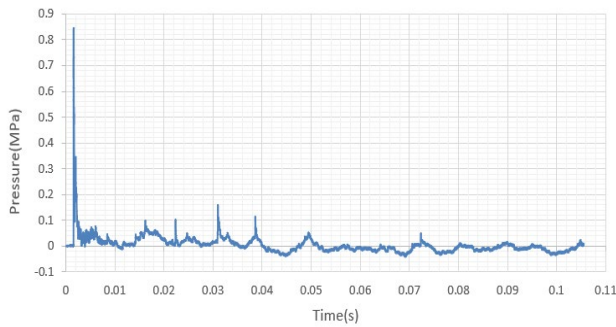


Figure 9. Pressure-time graph of the explosion of 1000 g of TNT at 2.5 m distance from the measurement wall

2.3. Evaluation of the data

After the blast, cracks were observed in the reinforced walls and the ceiling of the reinforced concrete room resulting from the blast pressure. Sketches of the cracks, which were drawn based on observations, are presented in Figures 10 and 11. It was observed that the cracks in the ceiling extended toward the reinforced walls due to the fact that the cracks in the tension zone on the ceiling expanded over time and the cracks in the compression zone were closed. The two cracks numbered 1 and 2 in Figures 10 and 11 were assessed, and it was found that the crack 1, measuring 1.5 m long and 0.7 mm wide, extended from the center of the ceiling toward the walls with the openings, while crack 2, measuring 0.75 m long and 0.3 mm wide, extended from the center of the ceiling toward the reinforced walls. It was observed that the pressure from the internal blast had forced the reinforced walls to rotate, causing cracks to form in the areas where they met the raft foundation, where a crack 0.5 m in length and 0.2 mm in width (crack 3 in Figure 10) was found. It was observed that a similar crack 3 m long and 1.3 mm wide had formed on the wall with the door opening (crack 4 in Figure 10). On the same wall, another crack (crack 5 in Figure 10) 1 m long and 0.5 mm wide, extending from the upper edge of the door toward the center was observed. In the area where the reinforced wall with the window opening met the raft foundation, cracks 6 shown in Figure 11 was 1.75 m long and 0.9 mm wide. In the same area, two cracks (cracks 7 in Figure 11) measuring 1 m in length and 0.5 mm in width, extending from the upper edges of the window opening toward the right and left walls, were found. In the area where the reinforced wall opposite the measurement wall met the raft foundation, cracks measuring 1 m long and 0.5 mm wide (cracks 8 in Figure 11) were observed. These cracks were longer and wider than the one noted on the measurement wall, which was attributed to the crack distribution on the ceiling. An examination of the distribution of cracks on the ceiling showed that the cracks extending toward the walls containing the door and window openings were longer. The results indicated that the measurement wall behaved more rigidly, causing the formation of fewer cracks.

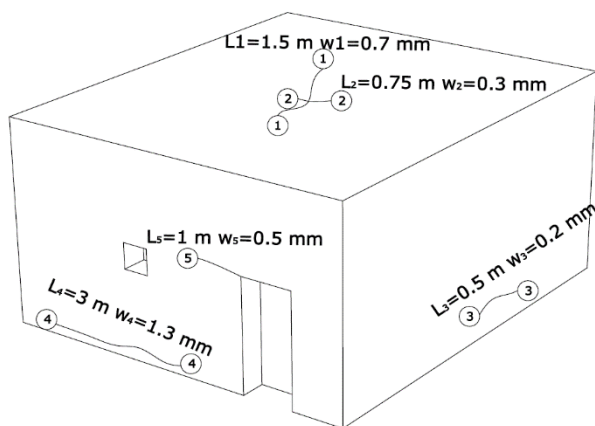


Figure 10. Sketch of cracks formed in the reinforced concrete room (front view)

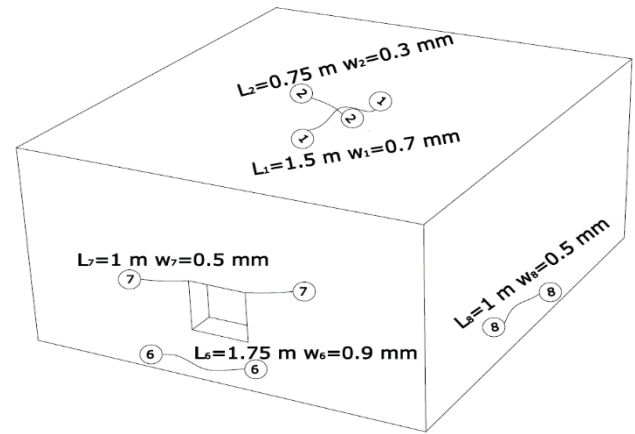


Figure 11. Sketch of cracks in the reinforced concrete room (rear view)

The theoretical correspondence of the data obtained from the experiment with the graphical data given in UFC 3-340-02 Structures to Resist the Effects of Accidental Explosions [5] and Cormie et al. [4] was investigated. Using Baker's [3] model, an assessment was made of the number of shock pressures and the change in pressure over time.

The Z value ($\text{m/kg}^{1/3}$) was calculated to be 2.5 $\text{m/kg}^{1/3}$, based on the variables in the experimental study. According to the graph developed by Cormie et al. [4], the pressure value was calculated to be 2.83 MPa. The maximum shock pressure recorded in the experiment was 0.84 MPa. An examination of the experimental data indicated that the maximum shock pressures calculated according to the graphs of Cormie et al. [4] were higher than the maximum shock pressure recorded in the present study. The variation between pressure values may be attributable to the openings in the structures and the differences in the volume of the structures.

UFC 3-340-02 Structures to Resist the Effects of Accidental Explosions [5] suggests the calculation of idealized shock pressure using graphs and the parameters identified based on the position of the explosive within the structure, the amount of explosive and the form of the structure. In the graphs given in UFC 3-340-02 Structures to Resist the Effects of Accidental Explosions [5], the maximum Z value is 4 $\text{ft/lb}^{1/3}$. This regulation suggests that in cases where values beyond the limit values are obtained, calculations should be made considering the limit values. In the present study, the Z value was calculated to be 6.30 $\text{ft/lb}^{1/3}$. Since the Z value of the explosive was above 4 $\text{ft/lb}^{1/3}$, the shock pressure idealized using the limit value of 4 $\text{ft/lb}^{1/3}$ was calculated to be 0.46 Mpa.

The three shock pressures in Baker's [3] approach were not observed in the pressure-time graph of the blast. Furthermore, unlike in Baker's approach, where it is assumed that the time between shock pressures is constant, the time between the pressure waves in the graph was found to be variable.

3. Theoretical Study

The theoretical study made use of the ABAQUS program, which is widely used for explosion and impact analyses. In order to shorten the number of operations and the time in the model, a linear hexagonal hedral 8-point box (C38DR) element with integrated integration was used for the concrete elements. A two-node beam member (B31) was used for reinforcement. The reinforced concrete room was modeled in 3D using ABAQUS 6.13.1, as shown in Figure 12. The wall with the observation window containing pressure-resistant glass was modeled as a reinforced wall; the measured wall was the number one building element; the wall with the door opening was the number two building element; the wall with the window opening was the number three building element; and the ceiling covering was the number four building element. The plastic damage parameters of the concrete were taken from studies in literature (Table 4) [13]. For the concrete pressure and tensile stresses, the models developed by Birtel and Mark [13] and Hordijk [14] were used, respectively. The TS-500 regulation was used for the elastic parameters of concrete [15]. The elasticity modulus of concrete was assumed to be 32,000 MPa, and Poisson's ratio was 0.20.

Equations 1 and 2 provided in the Abaqus documents were used for the calculation of the compressive and tensile damage to the concrete [16]. The contact has been provided between the elements by determining the surface on the joint. It was determined that it would be appropriate to use 100x100x100 mm hex mesh by conducting a convergence study on the elements. An hourglass control was carried out to prevent any unreal deformations. The analysis was completed in approximately 114 hours by a 2.60 GHz and 16 GB memory 7-core computer.

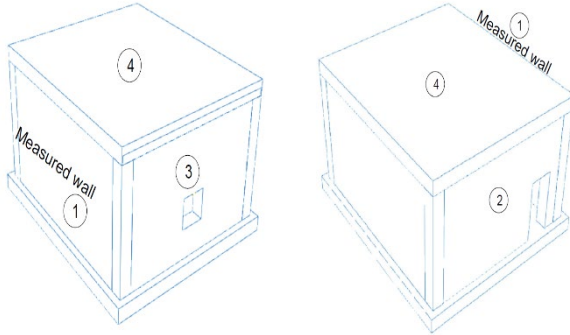


Figure 12. (a) Front view of the Abaqus model; (b) Rear view of the Abaqus model

Table 2. Plastic damage parameters [13]

Dilation Angle (ψ)	Ratio of Biaxial to Uniaxial Compressive Strength (α_f)	Flow Potential (ϵ)	Second Stress Invariant Ratio (K_c)
30°	1.16	0.1	0.67

The equations in the Abaqus documents were used for the calculation of the tensile (d_t) and compressive (d_c) damage parameters of the concrete [16].

$$\sigma_t = (1 - d_t)E_0(\epsilon_t - \epsilon_t^{pl}) \quad \text{Equ. 1}$$

$$\sigma_c = (1 - d_c)E_0(\epsilon_c - \epsilon_c^{pl}) \quad \text{Equ. 2}$$

The pressures measured at one wall during the blast experiment carried out in the reinforced concrete room were applied to a four wall and ceiling model created using Abaqus software, and subjected to a dynamic explicit analysis. The pressures recorded in the experiment were applied uniformly to the elements of the structure on the basis of the assumptions in UFC 3-340-02 Structures to Resist the Effects of Accidental Explosions [5]. The effects of the blast pressure on the behavior of the structure with an average time of 0.1 s are given in Figures 14–17. An examination of the graphs shows that the maximum displacement resulting from the explosion was 0.59 mm at the center of the measurement wall, -0.75 mm at the center of the wall with the window opening, -0.66 mm at the center of the wall with the door opening and 1.27 mm at the center of the ceiling.

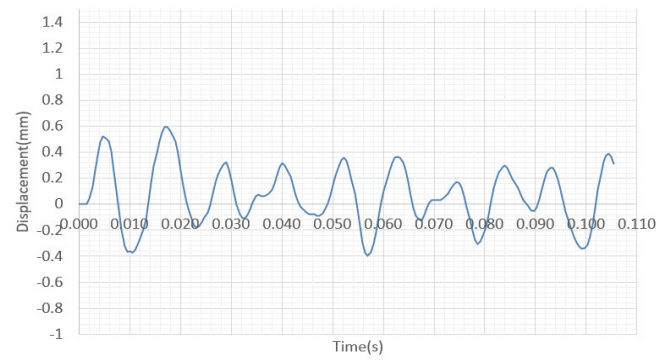


Figure 13. Graph showing the displacement at the center of the measurement wall vs. time (building element number 1)

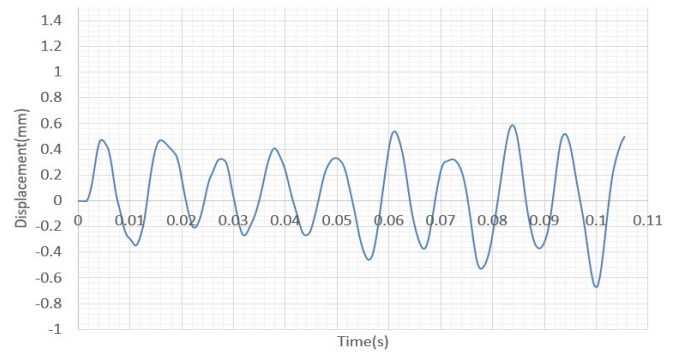


Figure 14. Graph showing the displacement at the center of the wall with the door opening vs. time (building element number 2)

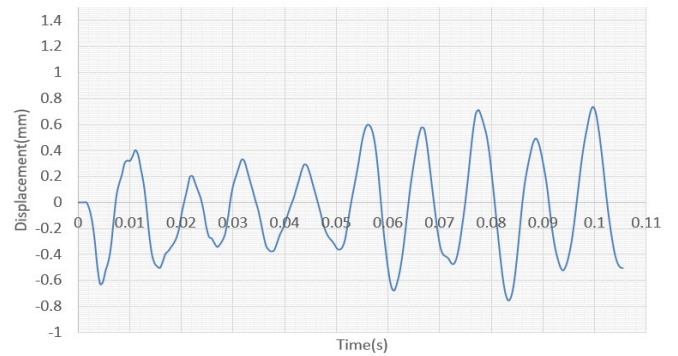


Figure 15. Graph showing the displacement at the center of the wall with the window opening vs. time (building element number 3)

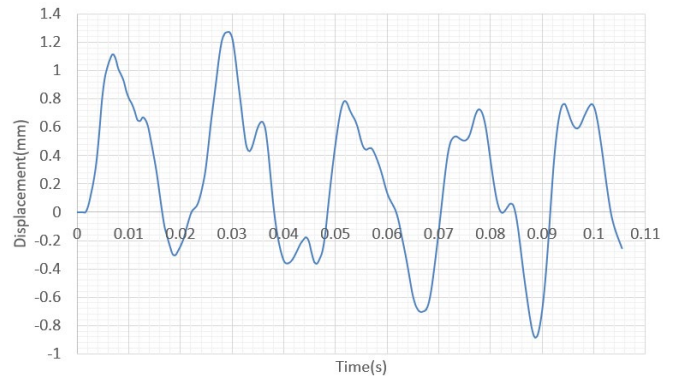


Figure 16. Graph showing the displacement at the center of the ceiling vs. time (building element number 4)

It was observed that the ceiling of the reinforced concrete room was affected more than the reinforced walls, which was attributable to the displacement of the tension and compression zones on the ceiling under the effect of the internal blast pressure.

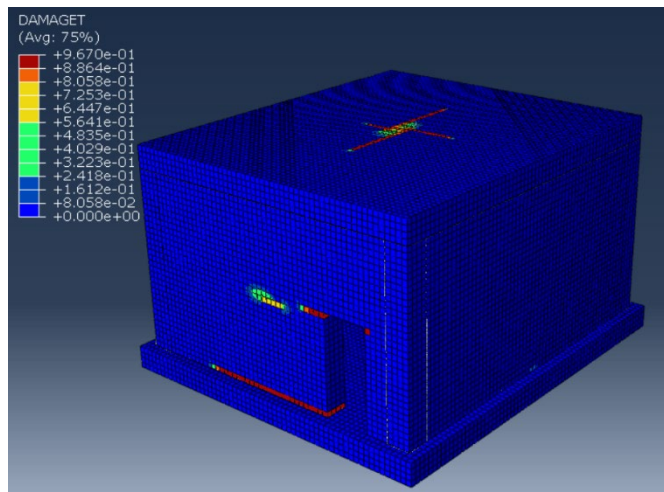


Figure 17. Tensile cracks on the elements of the reinforced concrete room (front view)

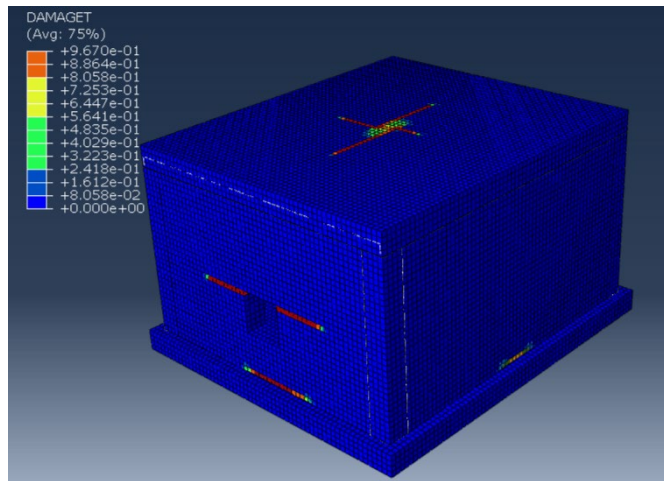


Figure 18. Tensile cracks on the elements of the reinforced concrete room (rear view)

The tensile cracks that formed on the elements of the reinforced concrete room are shown in Figures 18 and 19. It was observed that the cracks in the ceiling extended toward the reinforced walls due to the fact that the cracks in the tension zone on the ceiling expanded over time and the cracks in the compression zone were closed. Furthermore, two cracks, measuring 1.625 m and 1 m in length, and extending toward the reinforced walls from the center of the ceiling, were noted. It was observed that the pressure from the internal blast had forced the reinforced walls to rotate, causing cracks to form in the areas where the reinforced walls met the floor. A 0.75 m long crack was noted in the area where the measurement wall met the raft foundation, while a crack that formed in the reinforced wall with the door opening measured 3.25 m in length. In the same area, another crack measuring 0.625 m in length and extending from the upper side of the door opening toward the center was noted. The length of the crack in the area where the reinforced wall with the window opening met the raft foundation was 2 m. In this area, a crack 1.25 m in length, extending from the upper edges of the window opening toward the right and left walls, was observed. A 1.25 m long crack was recorded in the area where the reinforced wall opposite the measurement wall met the raft foundation.

In the static analysis, all elements of the structure were modeled with a size of 50x50 cm, considering the maximum pressure force obtained

from the experimental study. The experimental maximum pressure force was divided into vector components and analyzed taking into account the component perpendicular to the center of each square piece. Since the maximum pressure force was measured using a piezoelectric pressure sensor on the measurement wall, it was applied to other elements of the structure after scaling with Z values. This method provided for a non-uniform load distribution across the elements of the structure. Figure 19 shows the diagram obtained by dividing the measurement wall into 50x50 cm square blocks.

1	5	9	13	17	21	25	25	21	17	13	9	5	1
2	6	10	14	18	22	26	26	22	18	14	10	6	2
3	7	11	15	19	23	27	27	23	19	15	11	7	3
4	8	12	16	20	24	28	28	24	20	16	12	8	4
4	8	12	16	20	24	28	28	24	20	16	12	8	4
3	7	11	15	19	23	27	27	23	19	15	11	7	3
2	6	10	14	18	22	26	26	22	18	14	10	6	2
1	5	9	13	17	21	25	25	21	17	13	9	5	1

Figure 19. Measurement wall divided into small square blocks

The displacement graphs for the structural elements, plotted based on the results of the static analysis, are presented in Figures 20-23. The maximum displacements obtained were -0.035 mm at the center of the measurement wall, 0.024 mm at the center of the reinforced wall with the door opening, 0.026 mm at the center of the wall with the window opening, and 0.046 mm at the center of the ceiling. In the static analysis, no crack formed in the reinforced concrete room, while in the dynamic analysis, cracks formed on the outer surface of the elements of the reinforced concrete room. Cracks to the outer surfaces of the reinforced walls and the ceiling formed due to the tensile stresses under dynamic loads. The reinforcement bars that best alleviated the tensile stresses on the outer surfaces of the elements of the reinforced concrete room under internal blast loads were those that were closest to the outer surface.

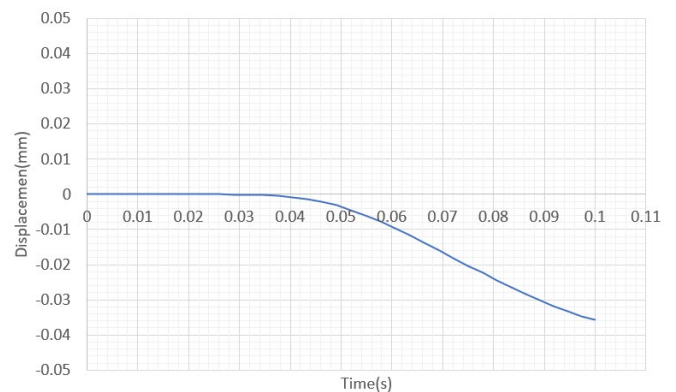


Figure 20. Graph of the displacement at the center of the measurement wall vs. time (building element number1)

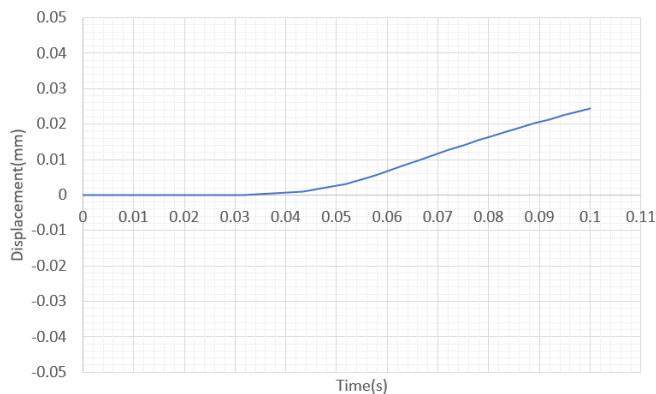


Figure 21. Graph of displacement at the center of the wall with the door opening vs. time (building element number2)

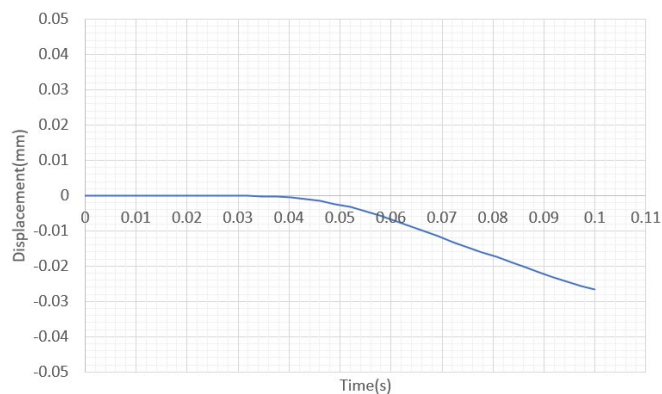


Figure 22. Graph of displacement at the center of the wall with the window opening vs. time (building element number3)

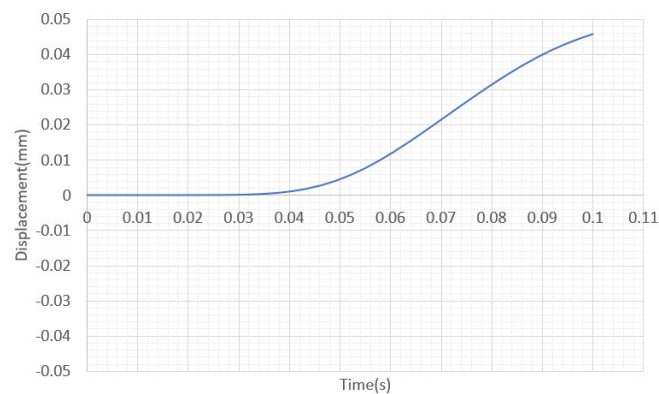


Figure 23. Graph of displacement at the center of the ceiling vs. time (building element number4)

In the analyses using the data obtained from the experiment, an attempt was made to ascertain the behavior of the different elements of the reinforced concrete room. The dynamic and static analyses showed that the maximum displacements at the center of the measurement wall resulting from the blast were 0.59 mm and -0.035 mm, respectively; that the maximum displacements at the center of the wall with the door opening due to the blast were 0.66 mm and 0.024 mm, respectively; that the maximum displacements at the center of the wall with the window opening due to the blast were -0.75 mm and 0.026 mm, respectively; and that the maximum displacements at the center of the ceiling were 1.27 mm and 0.046 mm, respectively. An examination of the displacement graphs of the structure obtained in the dynamic analysis indicated that the elements of the reinforced concrete room sprang, with the generated energy being absorbed by the structure.

4. CONCLUSION

A pressure-time graph was obtained based on the blast experiment results showing that the pressure lasted for 0.105 s, and that the first pressure wave reached the measurement wall in 0.00018 s. The maximum shock pressure measured using the piezoelectric pressure sensor was 0.84 Mpa, occurring 0.0016 s after the blast. As a result of the blast, no rupture or permanent deformation was observed on the inner or outer surfaces of the elements of the reinforced concrete room, although cracks had formed on the surfaces. The length and width of each crack that formed on the reinforced concrete room elements due to the blast were measured.

The static and dynamic solutions produced based on the structural behavior recorded during the experiment, and according to international standards and regulations, were evaluated.

The sketches of the cracks drawn based on the observations made after the experiment were compared with those obtained from the theoretical study.

- No crack was observed in the static analysis, whereas the sketch of the cracks made following the dynamic analysis resembled the one drawn based on the observations made after the experiment.
- A comparison of the locations, forms and lengths of the cracks that formed due to the blast with those obtained from the dynamic analysis showed that the locations and forms were similar, whereas the cracks obtained in the dynamic analysis were longer and created permanent deformations.

The pressure calculated based on the graphs developed by Cormie et al. was 2.84 Mpa, while the pressure calculated based on the UFC 3-340-02 Structures to Resist the Effects of Accidental Explosions was 0.46 Mpa. The pressure value recorded in the experimental study differed in magnitude from that calculated based on the models of Cormie et al. and presented in UFC 3-340-02 Structures to Resist the Effects of Accidental Explosions.

The variation between the maximum shock pressure value obtained from the experimental study and the maximum shock pressure value, calculated based on the model of Cormie et al., may be attributed to the openings in the structure.

The difference between the maximum shock pressure value obtained from the experimental study and the maximum shock pressure value based on UFC 3-340-02 Structures to Resist the Effects of Accidental Explosions may be due to the calculation of pressure using the limit value, since the Z value in the experiment data was greater than the limit value, i.e. 4 ft/lb^{1/2}, in the UFC 3-340-02 Structures to Resist the Effects of Accidental Explosions.

In the experimental blast, the largest crack was expected to form on the measurement wall, however more cracks were observed in the reinforced walls containing the openings. It would normally be expected for the shock waves to erupt out of the door and window openings, and to inflict less damage to these walls. However, more cracks formed in the walls containing the door and window openings, as the openings reduced the rigidity of the walls. The displacement graphs obtained from the dynamic analysis demonstrate that the maximum displacement occurred on the ceiling. The displacements at the centers of the reinforced walls containing the door and window openings were greater than those recorded at the center of the measurement wall. These results are in line with the experiment data, and suggest that the effects of the openings on the building elements on the behavior of the structure were clearly determined, both in the experimental study and in the dynamic analysis.

The static analysis revealed that the maximum displacement occurred on the ceiling, while the displacements in the reinforced walls containing the openings were less than in the measurement wall. This may be attributed to the method employed for the static analysis, and to the fact that the dynamic effect was converted into a static effect.

The measured displacements obtained from the static analysis were 3–6% of those obtained from the dynamic analysis. The results obtained from the static analysis suggest that the results of the

dynamic analysis are consistent with the data from the blast experiment.

Nomenclature

σ_t : Tensile stress

σ_c : Compression stress

d_t : Tensile damage parameter

d_c : Compression damage parameter

E_o : Initial elastic stiffness of the material

ε_t : Strain under tension

ε_c : Strain under compression

ε_t^{pl} : Plastic strain under tension

ε_c^{pl} : Plastic strain under compression

Declaration of Conflict of Interests

The authors declare no conflict of interest.

References

- [1.] Beshara F.B.A. Modelling of blast loading on aboveground structures-II. Internal blast and ground shock. Computers & Structures (1994), Vol. 51, No 5, pp. 597-606.
- [2.] US Army Corps of Engineers, Naval Facilities Engineering Command, Air Force Civil Engineer Support Agency. Design and analysis of hardened structures to conventional weapons effects. UFC 3-340-01. Supersedes TM5-855-1/NAVFACP-080/AFJAM32-1055/DSWA DAHSCWEMAN-97 August 1998. US Army Corps of Engineers and Defense Special Weapons Agency, Washington, DC, (2002).
- [3.] Baker, W. E., Cox, P. A., Westine, P. S., Kulesz, J. J. Strehlow, Fundamental studies in engineering. In Explosion hazards and evaluation. Vol. 5, Amsterdam, Oxford, New York: Elsevier. (1983). ISBN: 0 444 420940.
- [4.] Cormie D., Smith P. and Mays G. Blast effect on buildings. Cranfield University at the Defence Academy of the United Kingdom, London, (2009). ISBN: 978-0-7277-3403-7.
- [5.] US Army Corps of Engineers, Naval Facilities Engineering Command, Air Force Civil Engineer Support Agency. Structures to resist the effects of accidental explosions. UFC 3-340-02. Supersedes TM 5-1300, November 1990. US Department of Defense, Washington, DC, (2008).
- [6.] Haskett M., Edri I., Savir Z., Feldgun V.R., Karinski Y.S., Yankelevsky D.Z., On blast pressure analysis due to a partially confined explosion: I. Experimental studies. International Journal of Protective Structures (2011), Vol.2, No 1, pp:1-20.
- [7.] Yao S., Zhanga D., Lu F., Chena X., Zhaob P., A combined experimental and numerical investigation on the scaling laws for steel box structures subjected to internal blast loading. International Journal of Impact Engineering 102 (2017), pp: 36-46.
- [8.] Yao S., Zhang D., Lu F., Dimensionless number for dynamic response analysis of box-shaped structures under internal blast loading. International Journal of Impact Engineering 98 (2016), pp: 13-18.
- [9.] Tai Y.S., Chu T.L., Hu H.T., Wu J.Y., Dynamic response of a reinforced concrete slab subjected to air blast load. Theoretical and Applied Fracture Mechanics 56 (2011), pp: 140-147.
- [10.] AASTP-1: Manual of NATO Safety Principles For the Storage of Military Ammunition and Explosives, NATO International Staff – Defense Investment Division, (2006).
- [11.] European Committee for Standardization (CEN) Eurocode 1: Actions on structures, Part 1-7: prEN 1991-1-7: General actions-Accidental actions, (2006).
- [12.] IS 4991: Criteria for blast resistant design of structures for explosions above ground [CED 39: Earthquake Engineering], (1968).
- [13.] Birtel V., Mark P., Parameterised Finite Element Modelling of RC Beam Shear Failure. (2006), ABAQUS Users' Conference.
- [14.] Alfarah B., López-Almansa F., Oller S., A new methodology for calculating damage variables evolution in plastic damage model for rc structures. Engineering Structures 132 (2017), pp: 70-86.
- [15.] Betonarme Yapıların Tasarım ve Yapım Kuralları, TS 500, Türk Standartları Enstitüsü, Ankara, (2000).
- [16.] Abaqus, Theoretical manual, Version 6.13.1., Abaqus Inc., Johnston, USA, (2013).

How to Cite This Article

Demirel, Y., Polat, Ö., Examination of Experimental and Theoretical Behavior of a Reinforced Concrete Room under Internal Explosion Loads, Civil Engineering Beyond Limits, 4 (2020), 20-27.